Coil Size and Geometric Field Quality in Short Model Dipoles for LHC

Z. Ang, L. Bottura, S. Russenschuck, A. Siemko, D. Tommasini, L. Walckiers
CERN, LHC Division, 1211 Geneva 23, Switzerland

***Abstract*—We have measured the magnetic field at room temperature and at 1.8 K on more than twenty, 1-m long, single aperture LHC superconducting dipole models. The magnets feature either a 5-block coil geometry or the baseline 6-block geometry foreseen for the LHC. Comparison of warm and cold measurements show that the coil geometry is essentially unchanged during cooldown. We have therefore used mechanical measurements taken on the coil and collars during assembly to estimate the azimuthal coil length. Based on these measurements we show here that the sensitivity of allowed harmonics on coil size is in good agreement with the prediction obtained from the numerical model used for designing the LHC magnets.**

I. Introduction

The main bending dipoles for the Large Hadron Collider (LHC) must satisfy strict requirements on the magnetic field quality in order to achieve the expected beam luminosity at collision energy. This translates to tight manufacturing tolerances and requires that all magnets are systematically tested during production and at the reception at CERN [1]. The LHC dipoles are manufactured assembling four superconducting coils in a support structure formed by laminated collars. The collared coil assembly is completed by an iron yoke and a leak-tight shrinking cylinder of stainless steel. One of the key parameters to be controlled during production is the geometry of the coils after assembly in the collars, and in particular the azimuthal length a of the coil layers. This is defined as the length of the arc between the coil midplane and the surface of the pole (see Fig. 1). This parameter depends mainly on the pole shims between the coil and the collars and on the collar deformation during assembly. Studies on the magnets at HERA [2] and SSC [3] have shown that variations of the geometric harmonics are strongly correlated with coil deformations. We have reported elsewhere a first analysis of the correlation between the estimated coil size and measured allowed harmonics in LHC dipole models [4]. Here we extend the analysis to a larger number of magnets, featuring different coil geometries and collar materials. As done in [4] we focus on the first allowed harmonics. A good control of the allowed harmonics is very important as they will produce systematic effects in the LHC.

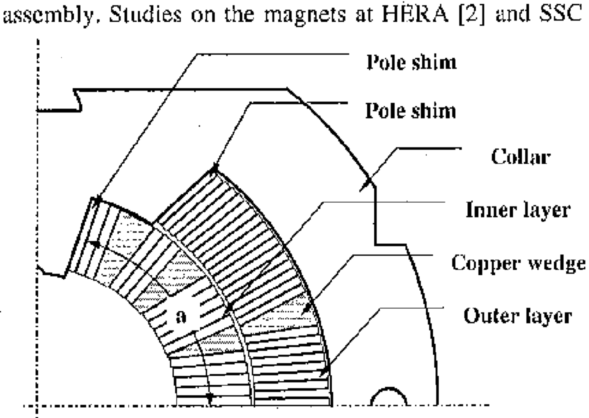

Fig. 1. Schematic geometry of a collared coil assembly (one quadrant), and definition of the azimuthal coil size a.

Manuscript received September 27, 1999

II. Series of Magnets Tested

The series of short models that are being manufactured at CERN within the frame of the R&D program for the LHC main dipoles [5] provides an ideal test-bed for correlation studies. A total of 21, 1-m long, single aperture magnets (the MBSMS series) and 5 twin aperture magnets (the MBSMT series) have been produced so far. The main purpose of the short model program is to explore the influence of manufacturing parameters on the quench performance and training behaviour. For this reason the coils of these magnets have been collared adjusting the pole shims to achieve coil compressions spanning a wide range, approximately 20 to 70 MPa after cool-down. Consequently the azimuthal length of the coils after collaring varied from magnet to magnet. This has given a good opportunity to study the dependence of the field harmonics on the coil size. The magnets considered here are the single aperture models MBSMS4 to MBSMS23 that we group in three families:

- magnets MBSMS4 through MBSMS13 constitute the first family. They are built using coils with 5 blocks of cables per quadrant (see Fig. 2) assembled into Al-alloy collars;
- the coil cross section has been modified as a result of optimization studies that have taken place during the R&D program. Magnets MBSMS15 through MBSMS23 feature the new optimized coil, with 6-cable blocks per quadrant (see again Fig. 2). About half of these magnets, our second family, have been assembled in Al-alloy collars (MBSMS15 through MBSMS18);
- the third family is formed by the remaining models, with 6-blocks coil geometry and austenitic steel collars. This family (MBSMS19 through MBSMS23) is at present the closest match to the baseline design of the main bending dipoles for LHC.

Several magnets were re-worked in different versions, changing the collaring and/or yoking conditions. In total we have performed magnetic measurements on approximately forty different magnets.

1051-8223/00$10.00 © 2000 IEEE

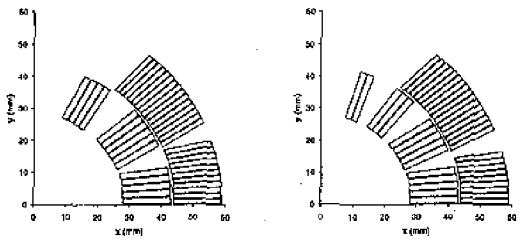

Fig. 2. Nominal geometry of one quadrant of the 5-blocks and 6-blocks dipole coils.

III. Field Quality Definitions

We follow standard practice in the description of the magnetic field B in accelerator magnets [6]. We ignore variations along the magnet length z and expand the field in the magnet cross-section x-y using the complex power series:

$$B(x, y) = B_y + iB_x = 10^{-4} B_1 \sum_{n=1}^{\infty} (b_n + ia_n) \left(\frac{x + iy}{R_{ref}} \right)^{n-1} \tag{1}$$

where B_1 is the dipole strength, R_{ref} is the reference radius (17 mm), b_n and a_n are the normal and skew $2n$-pole coefficients. In accordance with the above definition the harmonic coefficients are quoted in dimensionless *units*. In this paper we report the harmonics in a reference frame where the dipole is purely normal. In this reference frame the only harmonics allowed by symmetry are the normal, odd coefficients. For the dipole component we will also quote normalized values in units, defined as follows:

$$b_1 = 10^4 \frac{B_1 - B_1^{nom}}{B_1^{nom}} \tag{2}$$

where B_1^{nom} is a *nominal* dipole field evaluated as the average of the measured values on all magnets of a same family. With the above definition the values of b_1 for each family are centered around the average field. We therefore neglect systematic differences among magnet families, concentrating on relative variations within the same family.

IV. Mechanical Measurements and Coil Size

The coils used for the series of the MBSMS magnets do not have the same azimuthal size because of small variations of cable size, insulation thickness, thickness of the copper wedges and curing conditions. In order to achieve the desired azimuthal pre-compression the pole shims have been adjusted from magnet to magnet. The basis for the adjustment of the pole shims is the relation between azimuthal compression and pole displacement established in a press. During collaring the coil is forced into the volume delimited by the collar structure. In the ideal case of infinitely rigid collars the azimuthal coil size would be simply given by $a = a_{nom} - \delta_{shim}$, where a_{nom} is the nominal azimuthal length and δ_{shim} is the difference between the thickness of the pole shim used during collaring and the ideal shim (positive in the case of a shim larger than nominal). In reality the collars are not infinitely rigid and deform elastically during collaring. The total deformation δ_{collar} under the residual pre-compression has been measured after collaring at the outer surface of the collars, in correspondence of the poles. This measurement has been used to correct the estimated coil size as follows:

$$a \approx a_{nom} - \delta_{shim} + \delta_{collar} / 2 \, . \tag{3}$$

The estimated azimuthal size difference $\delta = a - a_{nom}$ ranges from 0.1 mm to 1 mm for the models with 5-blocks coils, and from –0.2 mm to 0.4 mm for those with 6-blocks coils.

TABLE I
Standard Deviation of the Correlation Between Warm and Cold Geometric Harmonics (in units @ 17 mm)

Order	5 blocks Al		6 blocks Al		6 blocks SS	
	$\sigma_{warm\text{-}cold}$		$\sigma_{warm\text{-}cold}$		$\sigma_{warm\text{-}cold}$	
	b_n	a_n	b_n	a_n	b_n	a_n
2	0.25	2.87	0.16	0.28	0.49	1.24
3	0.82	0.62	0.50	0.60	0.89	1.21
4	0.26		0.07	0.07	0.30	0.74
5	0.47		0.11	0.13	0.36	0.74

V. Magnetic Measurements

The warm and cold (1.8 K) measurements of the dipole model magnets are performed in a vertical test set-up, described in detail elsewhere [7]. The field is measured using radial coils mounted on a glass-fibre shaft rotating in the bore of the magnet. Five adjacent coils sections are installed to measure the field dependence along the magnet bore. Three 200 mm long coil sections cover the straight part. As we have done in our earlier study [4], we will refer here to the results from the centermost coil for the dipole component of the field, while the higher order harmonics will be given as dipole-weighted averages over the straight part. The cold testing procedure started with a standard pre-cycle (ramp-up to 11.75 kA and down to 50 A) to achieve a known and reproducible initial state. We have then ramped the current in steps and taken measurements at constant current at approximately 20 current values on both ramp-up and ramp-down powering branches. The geometric harmonics have been computed as the average of the measured values on the ramp-up and ramp-down branches at 5 kA [4]. Warm measurements were performed using the same test equipment, at 30 A current in the magnet. Positive and negative current measurements were taken to eliminate residual magnetization effects that can be significant at the small field level used during warm testing.

As reported in our previous work [4] there is a good correlation between the allowed harmonics measured in warm conditions and the geometric value in cold conditions. We strengthen our statement showing in Figs. 3 and 4 the scatter plot of warm and cold geometric sextupole and decapole for all single aperture models tested. The correlation is excellent and demonstrates that the thermal contraction during cool-down has no influence on allowed harmonics. In Table I we report the standard deviation of the warm-cold correlations, $\sigma_{warm\text{-}cold}$ defined as in [4], for the three families of magnets. This quantity gives an estimate of the typical

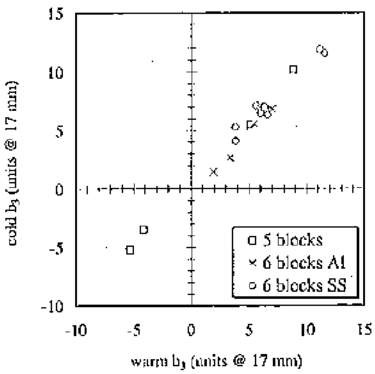

Fig. 3. Scatter plot of normal sextupole measured in warm and cold conditions (geometric component only).

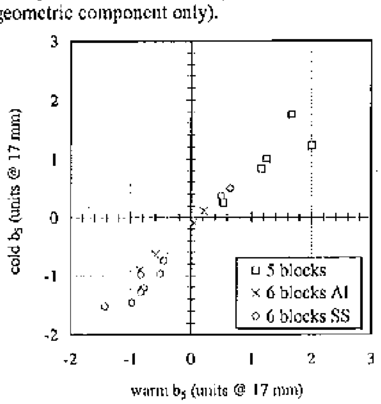

Fig. 4. Scatter plot of normal decapole measured in warm and cold conditions (geometric component only).

range of coil geometry control that can be achieved during series production of the dipoles, if warm measurements only are used to provide feed-back. We see there, as also evident from Figs. 3 and 4, that for allowed harmonics there is in practice no difference for different coil cross-sections or collar material. The variance observed on the non-allowed harmonics (in particular a_2) could be the result of a statistical anomaly due to the small number of tests (four) performed on Al-collars 6-blocks magnets.

VI. Field Calculation and Reconstruction

For the calculation of the effect of the azimuthal deformation of the coil we have used the analytical model of ROXIE [8]. We have assumed that the coil deformation takes place only in the cables, and that the copper wedges between blocks behave rigidly. A change of coil size in the azimuthal direction has been simulated stretching the width of the cables by a fixed amount. The total displacement δ of the pole surface was the result of the cumulative addition of the changes of the width of the cables in a layer. The result of this calculation is the set of harmonics $b_n^{def} + ia_n^{def}$ for the deformed coil. We have compared these values to the harmonics of the coil at nominal size b_n^{nom} ● ia_n^{nom} and we have computed the gradient (Jacobian) of the allowed harmonics with respect to the displacement:

TABLE II
Harmonics Jacobians for an Azimuthal Displacement of the Pole Surface (in units @ 17 mm/mm displacement)

Order	5 blocks coil		6 blocks coil	
	Inner layer	Outer layer	Inner layer	Outer layer
b_1	-54	-41	-55	-42
b_3	-16.1	-13.5	-17.2	-12.5
b_5	3.6	0.52	3.6	0.7
b_7	-1.7	0.16	-1.3	0.14
b_9	0.97	-0.02	0.48	-0.02

$$\frac{\partial b_n}{\partial \delta} \approx \frac{b_n^{def} - b_n^{nom}}{\delta}. \tag{4}$$

This gradient quantifies the sensitivity of the harmonic b_n to azimuthal coil size variations. Separate calculations were performed for the inner and outer layer, and for different amplitudes of displacement of the pole to confirm that for small displacements the relation between pole displacement and allowed harmonics is linear. The results of these simulations are summarized in Table II, where we report the Jacobians of the transfer function and of allowed harmonics with respect to a symmetric, outward displacement of all the pole surfaces in azimuthal direction. As expected, low order harmonics are the most affected. In addition the low order harmonics of both coil geometries depend strongly on both inner and outer layer size, while higher order harmonics are only sensitive to variations of the inner layer size. Comparing the values in Table II we remark finally that, apart for b_9, the Jacobians for the two coil types are essentially the same.

We have computed the geometric harmonics of all magnets tested using the estimated coil size of inner and outer layer, δ_{inner} and δ_{outer} respectively, and the Jacobians from Table I:

$$b_n = b_n^{nom} + \delta_{inner} \left.\frac{\partial b_n}{\partial \delta}\right|_{inner} + \delta_{outer} \left.\frac{\partial b_n}{\partial \delta}\right|_{outer}. \tag{5}$$

The computed geometric dipole, sextupole and decapole are compared in Figs. 5, 6 and 7 to the geometric values measured in cold conditions. The reconstruction agrees satisfactorily with the measurements. To quantify the quality of the correlation we have fitted each family of magnets with an ideal correlation line (unit slope) and adjusted offset Δ_{calc}. The values of the offsets for the three families of magnets are reported in Table III. Note that in accordance with the definition of the dipole variation given by (2) we have neglected systematic offsets on b_1. For this reason dipole offsets are not reported in Table III.

For an ideal correlation we expect $\Delta_{calc} = 0$. A value different from zero points to systematic effects that have not been taken into account in the reconstruction. We see in Table III and in Fig. 6 that for the sextupole there is a clear trend of decreasing offset Δ_{calc} in going from 5 blocks coils to 6 blocks coils, and further from Al-alloy to austenitic steel collars. We believe that the offset is largely due to an additional systematic deformation of the collars during assembly. This deformation results in a deviation of the final coil geometry from the nominal one. The effect is stronger if Al is used as collar material because its elastic modulus is smaller than that of austenitic steel. A similar behaviour is observed for b_5, b_7 and b_9 (see Table III). In this respect steel collars are superior as the final coil geometry is closer to the nominal one.

A second quantity of interest is the spread around the ideal correlation line. We quantify this spread using the standard deviation around the fit line σ_{calc}, defined as in [4] and reported in Table III for the three families. This quantity gives an overall measure of random variations from magnet to magnet that can be associated with uncertainties in the reconstruction, changes of manufacturing parameters (e.g. coil pre-stress) or components (e.g. different radial shims). It is therefore representative of the typical control that can be achieved throughout a production once systematic effects are corrected. The three families do not show particular differences in this respect. Note that in our case large geometry variations were planned from the start of the production of the model dipoles, therefore the values of σ_{calc} quoted in Table III should be regarded as a conservative upper bound of the standard deviation for the series production of the LHC dipoles.

VII. Conclusions

In the LHC magnets the azimuthal coil size after collaring, in warm conditions, correlates well with allowed geometric harmonics measured in cold conditions at 5 kA excitation current. This is a direct consequence of the fact that irrespective of the coil geometry or collar material the coil geometry is not deformed during cool-down, except for a uniform thermal shrinkage. The sensitivity of the geometric harmonics to azimuthal size variations can be predicted accurately using an analytical model. Examining the three families of models tested it can be seen that a clear advantage of austenitic steel collars is that the coil geometry of the finished magnet is closer to the nominal one owing to the larger structural rigidity of steel.

References

[1] L. Walckiers et al., "Towards series measurements of the LHC superconducting dipole magnets", Proc. of 1997 Part. Acc. Conf., Vancouver, pp. 3377-3379, 1997.

[2] K.-H. Mess, P. Schmueser, S. Wolf, Superconducting Accelerator Magnets, *World Scientific*, 1996.

[3] T. Ogitsu, A. Devred, "Influence of azimuthal coil size variations on magnetic field harmonics of superconducting particle accelerator magnets", *Rev. Sci. Inst.*, vol. 65 (6), pp. 1998-2005, 1994.

[4] Z. Ang, L. Bottura, D. Tommasini, L. Walckiers, "Magnetic field quality of short superconducting dipole model magnets for LHC", Proc. of 15th Int. Mag. Tech. Conf., pp. 145-148, 1997.

[5] N. Andreev et al., "The 1-m long simple aperture dipole coil test program for LHC", Proc. of 1996 European Part. Acc. Conf., Sitges, pp. 2258-2260, 1996.

[6] R.A. Beth, "Complex representation and computation of two-dimensional magnetic fields", *J. Appl. Phys.*, vol. 37 (7), pp. 2568-2571, 1966.

[7] Z. Ang, I. Bejar, L. Bottura, D. Richter, M. Sheehan, L. Walckiers, R. Wolf, "Measurement of AC loss and magnetic field during ramps in the LHC model dipoles", *IEEE Trans. Appl. Sup.*, vol. 9 (2), pp.742-745, 1999.

[8] ROXIE: Routine for the optimization of magnet X-sections, inverse field calculation and coil end design, S. Russenschuck ed., CERN Yellow Report 99-01, 1999.

TABLE III
Offset and Standard Deviation of The Correlation between Geometric Harmonics and Reconstruction (in units at 17 mm)

Order	5 blocks Al		6 blocks Al		6 blocks SS	
	Δ_{calc}	σ_{calc}	Δ_{calc}	σ_{calc}	Δ_{calc}	σ_{calc}
1		7.0		22.9		15.5
3	14.5±0.9	2.9	10.5±0.5	1.6	4.5±0.9	2.5
5	0.4±0.3	1.0	-1.0±0.1	0.4	0±0.1	0.4
7	0.7±0.07	0.2	0.5±0.1	0.3	0.2±0.05	0.2
9	-0.2±0.06	0.2	-0.1±0.02	0.1	-0.06±0.01	0.04

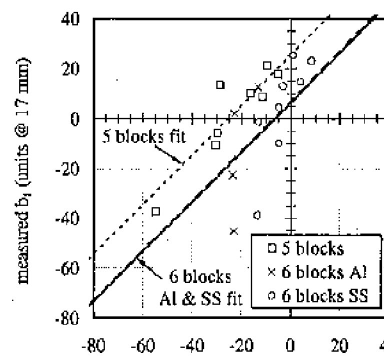

Fig. 5. Scatter plot of the variation of normal dipole measured and reconstructed by calculation in all models tested.

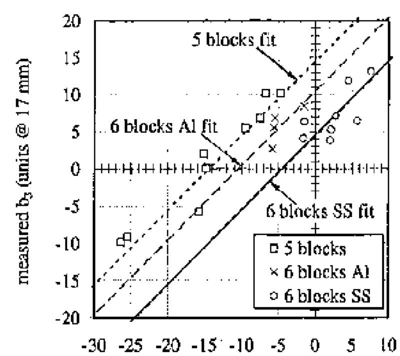

Fig. 6. Scatter plot of measured and reconstructed b_3.

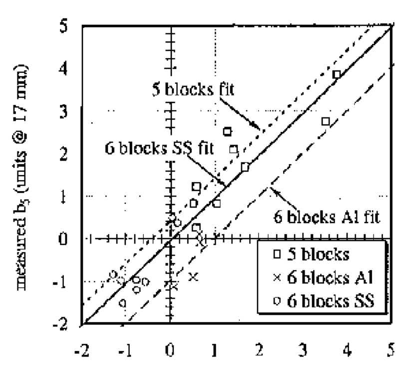

Fig. 7. Scatter plot of measured and reconstructed b_5.